Evaluation of a method to reduce uncertainty in wind hindcasts performed with regional atmosphere models

R. Weisse [a,*], F. Feser [a]

[a] *GKSS Research Center, Institute for Coastal Research, Max-Planck-Str. 1, 21502 Geesthacht, Germany*

Abstract

For more and more applications in coastal and offshore engineering numerical simulations of waves and surges are required. An important input parameter for such simulations are the wind fields. They represent one of the major sources for uncertainties in wave and surge simulations. Wind fields for such simulations are frequently obtained from numerical hindcasts with regional atmospheric models. The skill of these atmospheric hindcasts depends among others on the quality of the forcing at the boundaries. Furthermore, results may vary due to uncertainties in the initial conditions. By comparing different existing approaches for forcing a regional atmospheric model it is shown that the models sensitivity to uncertainties in the initial conditions may be reduced when a more sophisticated approach is used that has been suggested recently. For a specific, although somewhat brief test period it is demonstrated that an improved hindcast skill for near surface wind fields is obtained when this approach is adopted. Consequences of the reduced uncertainty in the wield fields for the hindcast skill of subsequent wave modelling studies are demonstrated. Recently this new approach has been used together with a regional atmosphere model to produce a 40-year wind hindcast for the Northeast Atlantic, the North Sea and the Baltic Sea. The hindcast is presently extended to other areas and the wind fields are used to produce 40-year high-resolution hindcasts of waves and surges for various European coastal areas.

Key words: near surface wind, ocean waves, wind and wave hindcast, North Sea, regional modelling

* Corresponding author.
Email addresses: weisse@gkss.de (R. Weisse), feser@gkss.de (F. Feser).

Article published in Coastal Engineering 48(4) pp.211-225, 2003

1 Introduction

Many applications in coastal and offshore engineering as well as in ocean modelling or for climate impact studies require detailed knowledge of the prevailing wind, wave and/or surge conditions at specific locations. Often such information is hardly available, either due to incomplete observational records or even due to a complete lack of observational data. In such cases hindcasts obtained from numerical models have become a frequently used tool as they may provide at least the best possible guess of the environmental conditions that may have been observed at given time and location. Therefore, hindcasts are often considered to be a substitute reality (e.g., Ewing et al. 1979; The WASA-Group 1998).

In many cases hindcasts are performed with the objective to reproduce specific events; that is, limited time periods are modelled in order to obtain information on e.g., the wind, wave and surge conditions within a particular storm that, for instance, may have caused large damages in particular areas. Examples of such hindcasts are the simulation of the so-called Halloween storm in 1991 (Cardone et al. 1996) or the simulation of the wave conditions that caused the abandonment of five yachts in the 1998 Sydney to Hobart yacht race and forced a further 66 boats to retire from the race (Greenslade 2001).

More recently, however, hindcast simulations have also been performed for longer time periods covering many decades of years (e.g., Günther et al. 1998; Cox and Swail 2001; Soares et al. 2002). The objective of these simulations is twofold: On the one hand they provide relatively homogeneous data records that are sufficiently long and that have sufficiently high spatial resolution in order to be used for design purposes or other statistical analyses. (For instance, the European project HIPOCAS [Hindcast of Dynamic Processes of the Coastal Areas of Europe] was set-up to provide a 40-year high-resolution data base of wind, waves and surges for European coastal areas [Weisse and Gayer 2000; Feser et al. 2001; Soares et al. 2002; Weisse et al. 2002]). Here the phrase *relatively homogeneous* refers to the fact that homogeneity has been improved by using a frozen state-of-the-art numerical model, but that there are still remaining sources of inhomogeneity such as increasing density of observations that may be used for data assimilation (e.g., Swail et al. 1998; Swail and Cox 2000). On the other hand such hindcast simulations are used as substitute reality in order to assess trends in storm, wave and surge conditions that may have occurred in the recent past (e.g., Günther et al. 1998; Wang and Swail 2001; Wang and Swail 2002; Debernhard et al. 2002).

The conclusions that can be drawn from hindcast simulations depend to a large extent on the quality of the wave and surge hindcast which in turn depends critically on the quality of the driving wind fields. For instance, for a fully developed sea wave heights approximately scale with the square of the wind speed (Tolman 1998) which implies that an error of about 10% in the driving wind speed will result in

an error of at least 20% in the hindcast wave height. This is confirmed by other independent studies which showed that uncertainties in the wind field have a large impact on predicted waves (e.g., Teixeira et al. 1995; Holthuijsen et al. 1996).

Wind fields to force numerical wave and surge hindcasts can be obtained in several ways and from different sources. For multi-decadal simulations, however, additional requirements regarding the quality of the wind fields have to be made. For instance, the wind fields should be free of any artificial trends. They should be homogeneous in time in order not to violate the statistics that may be obtained from the wave/surge model simulations. Furthermore, for coastal applications the spatial and the time resolution of the wind fields should be high enough to resolve the relevant topographic features of the coastline in order to obtain appropriate wave/surge model simulations.

So far, the number of wind data sets fulfilling these requirements is rather limited. Presently relatively homogeneous wind fields can be obtained, for instance, from the so-called re-analyses projects (e.g., Kalnay et al. 1996; Gibson et al. 1996) for the past 15 to 40 years. In these projects global atmospheric circulation models (GCMs) have been used for re-analyzing observational data back in time for some decades using a frozen state-of-the-art data assimilation scheme together with an enhanced observational data base which additionally comprises observations which were not available in real time. In this way, global atmospheric data sets are generated that are considered to be much more homogeneous than any other global products available so far. Presently such global re-analyses have typical spatial resolutions of about 200 km and wind fields are provided every 6 hours.

While such global re-analyses provide a useful product for a variety of studies (e.g., climate studies), their spatial and temporal resolution remains too coarse for many environmental applications, such as ocean or wave modelling in coastal areas. Cox et al. (1995) have suggested an approach called *interactive objective kinematic analysis* (IOKA) to obtain high-quality and high-resolution wind fields from global or coarse resolution weather analyses or re-analyses. The approach is based on a manual interaction with an objective analysis system and has been proven to provide good results for many wave modelling studies (e.g., Swail and Cox 2000; Caires et al. 2002).

Due to the intensive manual part IOKA may become prohibitively expensive and time consuming. In addition, many applications such as surge modelling (e.g., Flather et al. 1998) or the reconstruction of atmospheric transports (e.g., von Storch et al. 2002) do require dynamically consistent fields of e.g., surface pressure, near-surface and upper level wind fields and/or temperature which are not provided by IOKA.

Therefore attempts have been made recently to use high-resolution regional atmospheric models (RAMs) driven by the re-analysis products at their lateral bound-

aries in order to obtain multi-decadal regional (wind) hindcasts that simulate the regional features in more detail (e.g., Feser et al. 2001). While the simulation of Feser et al. (2001) focuses on the North and Baltic Sea, similar simulations are being performed now for other European coastal areas (Soares et al. 2002).

A problem with such simulations is the internal model variability inherent in the RAMs (hereafter referred to as *inherent model uncertainty*); that is, small uncertainties in the initial conditions may sometimes accumulate to large differences during the integration. In other words, if two simulations are performed with only slightly different initial conditions the results of the two integrations may differ to a large extend after some time. While this behaviour is well-known for GCMs it has been acknowledged only recently for RAMs (e.g., Ji and Venrnekar 1997; Rinke and Dethloff 2000; Weisse et al. 2000; Weisse and Schneggenburger 2002).

For forecasting purposes the uncertainty resulting from this behaviour is usually assessed using ensemble simulations (e.g., Molteni et al. 1996). For hindcast simulations the assimilation of observed data may help to keep the model trajectory closer to the observations. For RAMs von Storch et al. (2000) suggested a method that could help to reduce the inherent model uncertainty in case that no further observational data are available for assimilation. They called this method *spectral nudging*. It is based on the idea that the trust or the *confidence* in the data derived from GCM simulations depends on the *spatial scale*; that is, features with horizontal scales smaller than a few hundred kilometres are usually not or at least less well resolved by the GCMs while large scale features such as the planetary scale circulation are well represented. In the spectral nudging approach suggested by von Storch et al. (2000) this additional information is fed into the RAM simulation. The spectral nudging approach may thus be considered as a simple approach to "assimilate" those scales of the global re-analysis in which one has the highest confi dence. Details are given in von Storch et al. (2000).

The objective of this paper is twofold: Keeping in mind the importance of the quality of the wind fi elds for wave and surge model simulations we fi rst investigate whether the spectral nudging approach is indeed capable of reducing the inherent model uncertainty in RAM hindcasts. This has not been addressed in von Storch et al. (2000). We then examine whether an improved hindcast skill can be obtained compared to hindcasts that use the conventional approach (that is, when spectral nudging is not used). We focus primarily on the uncertainty for wind fi elds. Additionally, we investigate the consequences for wave hindcasts driven by RAM winds. The paper is structured as follows: In section 2 we briefly describe the RAM and the wave model used for our study. Additionally, the experiments that have been performed are described. Section 3 is dedicated to the analysis of the model results and to the comparison with observations. Our results are assessed and discussed in section 4.

2 Models and Experiments

2.1 The Regional Atmosphere Model

For the wind hindcasts the regional atmosphere model REMO was used. The model is described in detail in Jacob et al. (1995) and Jacob and Podzun (1997). The model and the model set-up are identical to that used by von Storch et al. (2000) for the implementation of spectral nudging. The model is based on the primitive equations and is formulated for a grid-point and terrain-following hybrid coordinate system. The prognostic variables are surface pressure, horizontal wind components, temperature, specific humidity and cloud water. Furthermore, a soil model is included to account for variations in soil temperature and water content.

For our experiments we use the same model domain as described by von Storch et al. (2000) (cf. their Figure 1). The integration area covers Europe and large parts of the Northeast North Atlantic. The model operates on rotated spherical coordinates in order to achieve a minimum distortion of the grid boxes. The horizontal resolution in all simulations is $0.5^\circ \times 0.5^\circ$ and a time step of 5 minutes was chosen.

2.2 Experiments with the Regional Atmosphere Model

Two sets of ensemble simulations for January 1993 were carried out. In the first set of integrations the boundary conditions were forced upon the REMO using the conventional approach (CTR). In the second set of integrations the spectral nudging technique was used (SPN). Within each set, the experiments differ slightly in their initial conditions to account for the internal variability of the RAM (e.g., Weisse et al. 2000; Rinke and Dethloff 2000; Weisse and Schneggenburger 2002). For each set 6 experiments were performed starting successively on 26, 27, 28, 29, 30, and 31 December 1992 at 0:00 UTC. In the following the analysis is presented for the period 1 to 31 January 1993.

In all experiments REMO was driven by the NCEP re-analyses (Kalnay et al. 1996). New boundary conditions were provided every 6 hours. The spatial resolution of the NCEP re-analyses is approximately 210 km ($1.875^\circ \times 1.875^\circ$). Since REMO operates on rotated spherical coordinates the coverage of the REMO model domain with NCEP grid boxes is inhomogeneous. The highest improvement in spatial resolution is achieved in the southern part of the integration area. On average, the horizontal resolution is enhanced by a factor of 1:16 (von Storch et al. 2000).

2.3 The Wave Model and Experiments

The wind fields obtained from the REMO experiments have been used to produce ensemble wave hindcasts using the third generation wave model WAM as described in The WAMDI-Group (1988). The model has been set-up as a nested system with a coarse grid covering the North Sea and large parts of the Northeast North Atlantic. The fine grid nested within the coarse grid covers the North Sea south of 56°N. For all wave model simulations the horizontal resolution is about 50 km for the coarse grid and 5.5 km for the fine grid. Details of the set-up can be obtained from Table 1. Further details are provided in Soares et al. (2002).

Using this set-up we have performed 12 experiments with the wave model WAM for the period 1 to 31 January 1993. For all simulations the wave model was initialized with a wind dependent spectrum as described in Günther et al. (1991). The simulations differ only in the wind fields applied. For the first 6 simulations we have used the 6 different wind fields that were obtained from the 6 REMO integrations that utilized the CTR approach. For the other 6 wave hindcasts the 6 different wind fields obtained from the REMO SPN simulations were applied. This way all differences in the wave model simulations may be interpreted as resulting from the variations in the driving wind fields only.

3 Results

3.1 Inherent Model Uncertainty

In this section we want to investigate the variability that emerges in the REMO and the wave model simulations as a result of only small differences in the initial conditions of the atmospheric simulations. This variability is hereafter referred to as *inherent model uncertainty* (IMU).

In order to assess the IMU, for each realization k within an ensemble (CTR, SPN) the the root-mean-square distance r with respect to the ensemble mean obtained from all members of the same ensemble was computed as a function of time

$$r_k(t) = \sqrt{\frac{1}{M}\sum_{i=1}^{M}(x_{ik}(t) - < x_i(t) >)^2}. \qquad (1)$$

Here t represents time, $i = 1 \ldots M$ are the grid points in the model domain, and $< \ldots >$ denotes ensemble averaging. For the RAM simulations x denotes sea level pressure (SLP) while for the wave model simulation x represents significant wave height (Hs).

The magnitude of the IMU as a function of time is illustrated in Figure 1. It can be inferred that both, periods with rather low (e.g., between 11 and 16 January) and periods with rather high IMU (e.g., between 5 and 8 January) do occur. Further it can be obtained that the internal variability is largest for the CTR ensemble while it appears to be strongly reduced for the SPN ensemble. We therefore conclude that the spectral nudging approach is in principle capable of reducing the IMU in hindcast simulations with regional models in case no further observational data are available for assimilation.

3.2 Differences in Hindcast Skill

The second question to address is whether the hindcast skill is in principle being improved for the SPN simulations. As a first step we investigated whether there are any systematic differences between the two ensembles. Therefore we computed the root-mean-square distance $\bar{r}$ between the ensemble means of the SPN and the CTR integrations

$$\bar{r}(t) = \sqrt{\frac{1}{M}\sum_{i=1}^{M}(< y_i(t) > - < x_i(t) >)^2}. \qquad (2)$$

Here $< y_i(t) >$ represents the ensemble average of the SPN simulations (SLP or Hs), $< x_i(t) >$ denotes the ensemble mean of the CTR experiments (SLP or Hs, respectively) and $i = 1 \ldots M$ are the grid points in the model domain.

The result of this exercise is shown in Figure 2. It can be inferred that systematic differences between both ensembles do occur. Comparing the magnitude of these differences with the variations between the individual realizations of the CTR ensemble (Figure 1) reveals that most of the time the systematic differences between the ensemble means are larger than the IMU within the CTR ensemble. In addition, the temporary high internal variability within the CTR ensemble indicates that temporary large deviations between the model results and the observations must be expected since it is not a priori clear which model trajectory is going to be realized if only one integration is performed. This both suggests that systematic differences in the hindcast skill between both ensembles do occur.

For the SPN approach the IMU was remarkably reduced in our simulations (Figure 1). However, the question remains whether the hindcast skill in the SPN simulations was improved compared to the CTR experiments. To elaborate on this we compared our results with observed wind and wave data from two locations (Ekofisk, 56.5°N 3.2°E; Scharhörn, 54.0°N 8.4°E). For both locations hourly wind data for January 1993 were available. In addition, for Ekofisk also hourly wave data have been available.

Figure 3 and 4 show the observed together with the simulated wind speed and wind direction for January 1993 at Ekofisk and Scharhörn. In general, a relatively good agreement between the observations and the simulations can be inferred for both, the conventional and the spectral nudging approach although some events, such as for example the wind speed of more than 30 ms^{-1} at 23:00 UTC on 13 January at Scharhörn, are neither reproduced by the SPN nor by the CTR simulations.

The increased IMU for the CTR simulations around 7 January (Figure 1) can also be recognized for the wind speed and wind direction at Ekofisk and Scharhörn. At Ekofisk most of the CTR simulations underestimate the observations by up to 9 ms^{-1}. The wind direction varies between about 150°and 230°and deviates from the observed direction by up to 100° (Figure 3a,b). At the same time the wind speed is overestimated by up to 10 ms^{-1} at Scharhörn (Figure 4a). Compared to that the simulations using the SPN approach perform remarkably better (Figure 3c,d and 4c,d). Additionally, the variability among the individual realizations is strongly reduced for the SPN experiments.

For wind speed the differences in hindcast skill between the CTR and the SPN simulations are elaborated in more detail in Table 2 in which several skill measures for the individual realizations are presented. It can be obtained that compared to the CTR integrations the root-mean-square error between the simulated and the observed wind speed was reduced significantly for all SPN simulations. Also the correlation between the observations and the simulations is higher for the SPN experiments. For the bias the picture is not that clear. However, the bias is rather sensitive on how the observations have been reduced to 10 m height. For Scharhörn the impact may not be that dramatic since the observations were taken at 11 m height above ground. At Ekofisk, however, the anemometer height was 85 m and the details of the algorithm used to reduce the wind speed to 10 m height may become important. We also computed the Brier-Score BS defined as

$$BS = 1 - R_{SPN}^{2} R_{CTR}^{-2}, \tag{3}$$

where R denotes the the root-mean-square error for the nudged and the control simulations respectively (Table 2). Any positive value of BS thus implies an improved hindcast skill for the SPN compared to the CTR simulations. For instance, a Brier-Score of 0.20 indicates that the mean-square error has been reduced by 20%. Thus, according to Table 2 at both stations each SPN realization is performing better than its CTR equivalent.

As the wave model results depend strongly on the driving wind fields the conclusions drawn from the atmospheric fields hold also for the wave fields. Figure 1 clearly shows the enhanced uncertainty in those wave model simulations that use wind fields from the REMO CTR simulations. This uncertainty is strongly reduced when wind fields from the SPN integrations are used. The differences in hindcast skill for the significant wave height at Ekofisk are shown in Table 3. For Scharhörn

no wave height observations were available. As for the wind speed it can be obtained that for the SPN simulations the root-mean-square error is reduced and the correlation is increased compared to those obtained for the CTR experiments. Also for the wave heights, the Brier score indicates that an improvement in hindcast skill was obtained when winds from the SPN ensemble were used to drive the wave model.

3.3 Differences at 7 January

We found that in our simulations the highest IMU and the largest differences between the CTR and SPN simulations occurred around 7 January. We, therefore, would like to illustrate the synoptic conditions that are responsible for these differences.

The increased wind and wave height variability in the CTR integrations is associated with, and can be explained by, variations in the atmospheric conditions around 7 January. Figure 5 shows the SLP for 00:00 UTC 7 January 1993 for two CTR simulations which show a rather good (upper left) and a rather poor (upper right) agreement with observations together with the SLP for a SPN simulation (lower left) and the SLP obtained from the routine analysis performed by the German Weather Service (DWD) (lower right). In general there appears to be a reasonable agreement among all simulations and the DWD analysis. However, details differ and a closer inspection reveals pronounced differences in this overall agreement. For instance, the high pressure system over the Iberian peninsula has a core pressure of about 1035 hPa in the DWD analysis. While this is well represented in all SPN simulations the position and the strength of this high pressure system varies largely in the CTR simulations where core pressures of more than 1040 hPa are found. Furthermore, in the DWD analysis strong pressure gradients prevail over the Eastern Baltic Sea. While such strong pressure gradients may be found in only some of the CTR experiments they are reasonably reproduced in all SPN simulations. For the North Sea the differences in pressure gradient and thus in wind speed at Scharhörn and Ekofi sk may be inferred from the differences in position of the 1015 and the 1020 hPa contour line. Again the SPN simulations show on average a better agreement with the DWD analysis and the uncertainty between the individual realizations is strongly reduced.

In order to demonstrate this in more detail Figure 6 and 7 show again the IMU for the REMO and the wave model simulations for the North Sea area where Ekofi sk and Scharhörn are located. For the CTR ensemble large differences in the position of the 1015 and the 1020 hPa contour line are obtained that are related to strong variations in the horizontal pressure gradients at Ekofi sk and Scharhörn. These variations in the pressure gradient together with variations in the position of the pressure centers are fi nally responsible for the observed differences in the simulated

wind speed described above. For the SPN ensemble these differences are hardly visible. The similar holds for the wave model hindcasts (Figure 7). The uncertainty in the wind speed and wind direction obtained from the REMO CTR experiments leads to strong variations in the observed wave height. These variations are remarkably reduced when the wind fields from the SPN simulations are used.

4 Summary and discussion

Many applications in offshore and coastal engineering require numerical simulations of waves or surges. Wind fields are an important input parameter for such simulations and they represent at the same time a major source of uncertainty. In this study we investigated whether this uncertainty may be reduced if a recently proposed approach by von Storch et al. (2000) is used for the production of the wind hindcasts and if the hindcast skill in these simulations could be improved. Further, the consequences of the improved wind hindcasts for wave model simulations were demonstrated.

The sensitivity of the simulated wind fields, and thus the uncertainty in the simulations depending on the initial conditions, was assessed using ensemble simulations for the period January 1993. In one ensemble the conventional approach was utilized in which the model is driven by boundary conditions at its lateral boundaries only. In the other ensemble the recently proposed spectral nudging approach (von Storch et al. 2000) was used in which additional information regarding the large scale atmospheric circulation is fed into the RAM. It was shown that most of the time the ensemble variability appears to be small for both ensembles. However, for some periods the ensemble variability (uncertainty) was strongly increased in the control ensemble while it remained small in the spectral nudging integrations.

In these situations there are several atmospheric states about equally likely to occur in the CTR integrations. Accordingly, the regional atmospheric model shows very different results for only slightly modified initial conditions. In the perspective of numerical multi-decadal hindcasts or historical reconstructions only the trajectory closest to the observed state is desired. For the CTR realizations, it is not clear whether this trajectory is going to be realized if only one integration can be performed. Using the SPN approach this uncertainty is strongly reduced.

For the examples shown in this paper it could be further demonstrated that for the SPN simulations the hindcast skill was improved for both, the winds and the wave model results. For multi-decadal hindcasts with regional atmospheric models ensemble simulations for the entire simulation period are not feasible. Our results suggest that for such hindcasts the SPN approach could provide an alternative to keep the models trajectory closer to the observed one in case no further data for data assimilation are available. Based on this experience the approach has recently

been utilized by Feser et al. (2001) to produce a high-resolution wind hindcast for the North Sea, the Baltic Sea and the Northeast Atlantic covering roughly the past 40 years. Feser et al. (2001) provided their wind fi elds hourly at a spatial resolution of about 50×50 km. Comparison of simulated and observed wind fi elds indicated that this way a reasonable and high resolution hourly wind data set covering many years could be produced (e.g., Weisse and Gayer 2000; Soares et al. 2002; Weisse et al. 2002). Presently, the approach is used to produce further multi-decadal wind hindcasts for other areas. Furthermore, these wind fi elds are used to produce multi-decadal simulations of waves and surges for a number of European coastal areas (Soares et al. 2002).

Although the additional computational resources required for the spectral nudging are minor compared with enhanced data assimilation schemes, data assimilation should be favoured in case additional observational data are available that have not been assimilated in the global analyses. In addition, our conclusions are based on the analysis of a short time period only. Further tests over a larger data set are required to fully assess the improvements obtained from the SPN approach. Furthermore, the improvement in hindcast skill that can be obtained by using the SPN approach for multi-decadal hindcasts strongly depends on how often periods of enhanced IMU do occur and on the typical duration and spatial extend of such events. From the material presented here we may not conclude on the frequency and the typical spatial scale of such events. Further analysis of longer ensemble simulations is required to fully assess this topic. There are, however, a few recent studies which indicate that such events may occur a little more frequent: Rinke and Dethloff (2000) investigated the sensitivity of a regional arctic climate model to its initial conditions and found that due to the weaker lateral boundary control compared with mid-latitude RAMs a pronounced sensitivity of the Arctic simulations to uncertainties in initial conditions occurred. They concluded that changes in the monthly mean atmospheric structures caused by internal processes were in the same order as those induced by inaccurate physical parameterizations. Weisse et al. (2000) and Weisse and Schneggenburger (2002) investigated the sensitivity of a coupled regional atmosphere-wave-model to different sea state dependent roughnesses and initial conditions. They found that the sensitivity to modifi ed momentum flux parameterizations was in the same order of magnitude as the internal variability caused by modifi ed initial conditions. Further, they reported prolonged periods of enhanced internal model variability, some of which lasted several days up to almost a month. A similar result was found by De Zolt (pers. comm. 2000) who ran a regional atmospheric model for the Mediterranean for the year 1996.

Summarizing, the spectral nudging approach appears to be capable to reduce the IMU without squeezing the realistic small scale variability and to improve the hindcast skill for surface winds. Based on the analysis of wind speeds at Ekofi sk and Scharhörn it is concluded that some indications do exist that the spectral nudging approach should be favoured instead of the conventional approach for such applications as multi-decadal hindcasts. Further studies are, however, needed to investigate

the frequency of events with high internal model variability in integrations using the conventional approach. Spectral nudging may be seen as a sub-optimal and indirect data assimilation technique (von Storch et al. 2000), depending on the quality of the global forcing fi elds. Here we have shown that it may represent a useful approach for regional multi-decadal hindcasts and climate reconstructions for which limited computational resources and no further observational data for assimilation are available.

Acknowledgements

We thank Daniela Jacob and Ralf Podzun for their help with REMO and Hans Luthardt for assistance with the NCEP data. Lennart Bengtsson provided the permission to use the REMO model. Eduardo Zorita, Hans von Storch, and Heinz Günther carefully read the manuscript. We are grateful for their comments. The work was funded partly by the European Union under EVK2-CT-1999-00038 (HIPOCAS) and the Helmholtz Gemeinschaft Deutscher Forschungszentren via the Lead (Pb) Project.

References

Caires, S., Sterl, A., Bidlot, J., Graham, N., Swail, V., 2002. Climatological assessment of reanalysis ocean data. In: 7th International workshop on wave hindcasting and forecasting. Banff, Alberta, Canada, pp. 1–12.

Cardone, V., Jensen, R., Resio, T., Swail, V., Cox, A., 1996. Evaluation of contemporary ocean wave models in rare extreme events: The ”Halloween Storm” of October 1991 and the ”Storm of the Century” of March 1993. J. Atmos. Oceanic Technol. 13, 198–230.

Cox, A., Greenwood, J., Cardone, V., Swail, V., 1995. An interactive objective kinematic analysis system. In: 4th International workshop on wave hindcasting and forecasting. Banff, Alberta, Canada, pp. 109–118.

Cox, A., Swail, V., 2001. A global wave hindcast over the period 1958-1997: Validation and climate assessment. J. Geophys. Res. 106 (C2), 2313–2329.

Debernhard, J., Sætra, Ø., Roed, L., 2002. Future wind, wave and storm surge climate in the Northern Seas. Climate Res. 23, 39–49.

Ewing, J., Weare, T., Worthington, B., 1979. Hindcast study of extreme wave conditions in the North Sea. J. Geophys. Res. 84 (C9), 5739–5747.

Feser, F., Weisse, R., von Storch, H., 2001. Multi-decadal atmospheric modeling for Europe yields multi-purpose data. Eos Transactions 82 (28), 305,310.

Flather, R., Smith, J., Richards, J., Bell, C., Blackman, D., 1998. Direct estimates of extreme storm surge elevations from a 40-year numerical model simulation and from observations. Global Atmos. Oc. System 6 (2), 165–176.

Gibson, R., Kålberg, P., Uppala, S., 1996. The ECMWF re-analysis (ERA) project. ECMWF Newsl. 73, 7–17.

Greenslade, D., 2001. A wave modelling study of the 1998 Sydney to Hobart yacht race. Aust. Met. Mag. 50, 53–63.

Günther, H., Hasselmann, S., Janssen, P., 1991. Wamodel Cycle 4. Tech. Rep. 4, Deutsches Klimarechenzentrum, Available from Deutsches Klimarechenzentrum, Bundesstr. 55, D-20146 Hamburg, Germany, 102pp.

Günther, H., Rosenthal, W., Stawarz, M., Carretero, J., Gomez, M., Lozano, I., Serrano, O., Reistad, M., 1998. The wave climate of the Northeast Atlantic over the period 1955-1994: The WASA wave hindcast. Global Atmos. Oc. System 6 (2), 121–164.

Holthuijsen, L., Booji, N., Bertotti, L., 1996. The propagation of wind errors through ocean wave hindcasts. J. Offshore Mech. and Arctic Eng. 118, 184–189.

Jacob, D., Podzun, R., 1997. Sensitivity studies with the regional climate model REMO. Meteorol. Atmos. Phys. 63, 119–129.

Jacob, D., Podzun, R., Claussen, M., 1995. REMO - a model for climate research and weather prediction. In: Proc. Internat. Workshop on Limited-Area and Variable Resolution Models. Beijing, China, pp. 273–278.

Ji, Y., Venrnekar, A., 1997. Simulation of the Asian Summer Monsoon of 1987 and 1988 with a regional model nested in a global GCM. J. Climate 10, 1965–1979.

Kalnay, E., Kanamitsu, M., Kistler, R., Collins, W., Deaven, D., Gandin, L., Iredell, M., Saha, S., White, G., Woollen, J., Zhu, Y., Chelliah, M., Ebisuzaki, W., Higgins, W., Janowiak, J., Mo, K., Ropelewski, C., Wang, J., Leetmaa, A., Reynolds, R., Jenne, R., Joseph, D., 1996. The NCEP/NCAR reanalysis project. 77 (3), 437–471.

Molteni, F., Buizza, R., Palmer, T., Petroliagis, T., 1996. The ECMWF ensemble prediction system. Quart. J. Roy. Meteor. Soc. 122 (529), 73–119.

Rinke, A., Dethloff, K., 2000. On the sensitivity of a regional Arctic climate model to initial and boundary conditions. Climate Res. 14 (2), 101–113.

Soares, C., Weisse, R., Carretero, J., Alvarez, E., 2002. A 40 years hindcast of wind, sea level and waves in European waters. In: Proceedings of OMAE 2002: 21st International Conference on Offshore Mechanics and Arctic Engineering 23-28 June 2002. Norway, Oslo.

Swail, V., Cardone, V., Cox, A., 1998. A long term North Atlantic wave hindcast. In: 5th International workshop on wave hindcasting and forecasting. Melbourne, Florida, USA, pp. 1–16.

Swail, V., Cox, A., 2000. On the use of NCEP/NCAR reanalysis surface marine wind fi eld s for a long term North Atlantic wave hindcast. J. Atmos. Oceanic Technol. 17, 532–545.

Teixeira, J., Abreu, M., Soares, C., 1995. Uncertainty of ocean wave hindcasts due to wind modelling. J. Offshore Mech. and Arctic Eng. 117, 294–297.

The WAMDI-Group, 1988. The WAM model - a third generation ocean wave prediction model. J. Phys. Oceanogr. 18, 1776–1810.

The WASA-Group, 1998. Changing waves and storms in the Northeast Atlantic? 79 (5), 741–760.

Tolman, H., 1998. Validation of NCEP's ocean winds for the use in wind wave models. Global Atmos. Oc. System 6 (3), 243–268.

von Storch, H., Hagner, C., Costa-Cabral, M., Feser, F., Pacyna, J., Pacyna, E., Kolb, S., 2002. Reassessing past European gasoline lead policies. Eos Transactions 83 (36), 393,399.

von Storch, H., Langenberg, H., Feser, F., 2000. A spectral nudging technique for dynamical downscaling purposes. Mon. Wea. Rev. 128 (10), 3664–3673.

Wang, X., Swail, V., 2001. Changes of extreme wave heights in the Northern Hemisphere Oceans and related atmospheric circulation regimes. J. Climate 14, 2204–2221.

Wang, X., Swail, V., 2002. Trends of atlantic wave extremes as simulated in a 40-yr wave hindcast using kinematically reanalyzed wind fi elds. J. Climate 15 (9), 1020–1035.

Weisse, R., Feser, F., Günther, H., 2002. A 40-year high-resolution wind and wave hindcast for the Southern North Sea. In: 7th International workshop on wave hindcasting and forecasting. Banff, Alberta, Canada, pp. 97–104.

Weisse, R., Gayer, G., 2000. An approach towards a 40-year high-resolution wave hindcast for the Southern North Sea. In: Proceedings, 6th International Workshop on Wave Hindcasting and Forecasting,. Monterey, California, USA, pp. 204–210.

Weisse, R., Heyen, H., von Storch, H., 2000. Sensitivity of a regional atmospheric model to a sea state dependent roughness and the need of ensemble calculations. Mon. Wea. Rev. 128 (10), 3631–3642.

Weisse, R., Schneggenburger, C., 2002. The effect of different sea state dependent roughness parameterizations on the sensitivity of the atmospheric circulation in a regional model. Mon. Wea. Rev. 130 (6), 1595–1602.

Table 1
Wave model set-up.

	Coarse Grid	Fine Grid
Southernmost latitude	38.00°N	51.00°N
Northernmost latitude	77.00°N	56.00°N
Westernmost longitude	30.00°W	-3.00°W
Easternmost longitude	45.00°E	10.50°E
longitudinal resolution	0.75°	0.10°
latitudinal resolution	0.50°	0.05°
time step	900 s	180 s

Table 2
Bias B in ms^{-1}, root-mean-square error R in ms^{-1}, and correlation C between the wind speed obtained from the $k = 1 \ldots 6$ simulations using the conventional (CTR) or the spectral nudging (SPN) approach and the observations at Scharhörn (54.0°N, 8.4°E) and Ekofisk (56.5°N, 3.2°E). In addition, the Brier Score $BS = 1 - R^2_{SPN} R^{-2}_{CTR}$ is provided.

	CTR, Scharhörn			SPN, Scharhörn				CTR, Ekofisk			SPN, Ekofisk			
k	B	R	C	B	R	C	BS	B	R	C	B	R	C	BS
1	0.17	3.39	0.70	-0.12	2.56	0.83	0.43	0.69	3.59	0.81	1.00	3.18	0.85	0.22
2	0.21	3.40	0.70	-0.16	2.62	0.83	0.40	0.71	3.59	0.81	1.07	3.21	0.85	0.20
3	0.25	3.48	0.69	-0.12	2.53	0.84	0.47	0.70	3.54	0.81	1.07	3.18	0.85	0.19
4	-0.05	2.94	0.78	-0.09	2.53	0.84	0.26	0.85	3.41	0.82	1.01	3.19	0.85	0.13
5	0.04	3.19	0.75	-0.09	2.54	0.83	0.37	0.85	3.46	0.82	1.02	3.18	0.85	0.15
6	0.15	2.82	0.79	-0.01	2.46	0.84	0.24	0.85	3.33	0.83	0.97	3.17	0.85	0.09

Table 3
Bias B in m, root-mean-square error R in m, and correlation C between the wave height obtained from the $k = 1 \ldots 6$ wave hindcasts using either the wind fields from the REMO CTR or the REMO SPN simulations and the observations at Ekofisk (56.5°N, 3.2°E). In addition, the Brier Score BS is provided.

	CTR			SPN			
	B	R	C	B	R	C	BS
1	0.60	1.23	0.87	0.60	1.03	0.91	0.30
2	0.62	1.25	0.87	0.63	1.05	0.91	0.28
3	0.61	1.24	0.87	0.63	1.04	0.81	0.29
4	0.61	1.21	0.88	0.61	1.05	0.91	0.25
5	0.62	1.22	0.88	0.61	1.03	0.91	0.29
6	0.62	1.19	0.88	0.59	1.04	0.91	0.23

Fig. 1. Root-mean-square (rms) distance for SLP in hPa (top) and Hs in m (bottom) between the individual realizations of the SPN ensemble and their ensemble mean (solid) and between the individual realizations of the CTR ensemble and their ensemble mean (dashed).

Fig. 2. Root-mean-square (rms) distance for SLP in hPa (top) and Hs in m (bottom) between the ensemble means of the SPN and the CTR ensemble.

Fig. 3. Observed (black) and simulated (red) wind speed (a, c) in ms^{-1} and wind direction in degrees (b, d) at Ekofisk. The upper two panels (a, b) show the CTR, the lower two panels (c, d) show the SPN simulations.

Fig. 4. Observed (black) and simulated (red) wind speed (a, c) in ms^{-1} and wind direction in degrees (b, d) at Scharh¨orn. The upper two panels (a, b) show the CTR, the lower two panels (c, d) show the SPN simulations.

Fig. 5. SLP in hPa for two REMO CTR (upper panel) and one REMO SPN (lower left panel) realizations at 00:00 UTC 7 January 1993 together with the SLP obtained from the routine analysis of the German Weather Service (lower right). The two solid black points in each panel indicate the positions of Ekofisk (northernmost point) and Scharh¨orn (southernmost point).

Fig. 6. SLP in hPa obtained from the REMO CTR (left) and the REMO SPN (right) simulations at 00:00 UTC 7 January 1993. Shown are the 1015 hPa (solid) and the 1020 hPa (dashed) contour lines from all 6 REMO CTR (left) and all 6 REMO SPN (right) simulations. Note that the differences are hardly visible for the SPN simulations. The two solid black points indicate the positions of Ekofisk (northernmost) and Scharh¨orn (southernmost point).

Fig. 7. Total Hs in m for the WAM CTR (upper) and the WAM SPN (lower) simulations at 00:00 UTC 7 January 1993. Shown are the 1.5 m (solid) and the 2.0 m (dashed) contour lines for all 6 WAM CTR (upper) and all 6 WAM SPN (lower) simulations.

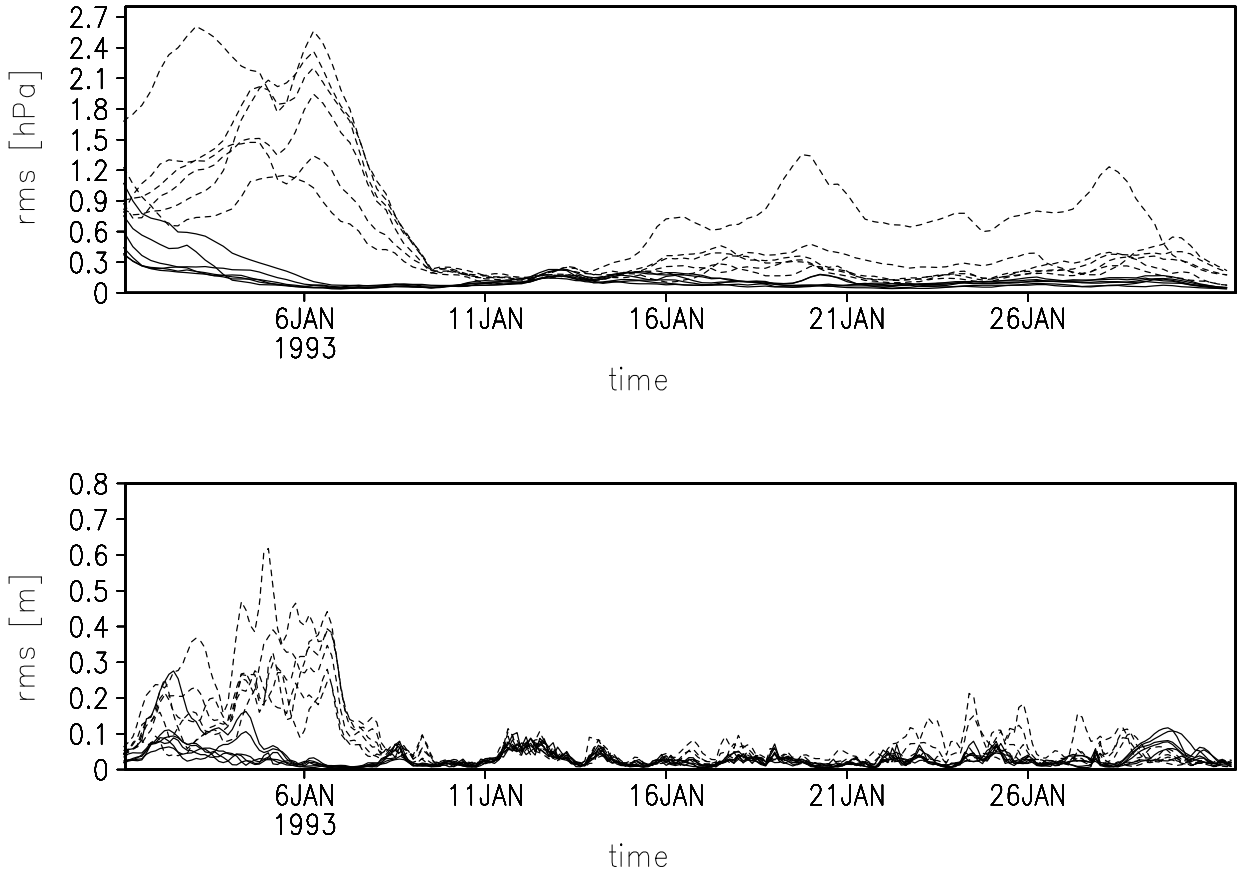

Fig. 1. Root-mean-square (rms) distance for SLP in hPa (top) and Hs in m (bottom) between the individual realizations of the SPN ensemble and their ensemble mean (solid) and between the individual realizations of the CTR ensemble and their ensemble mean (dashed).

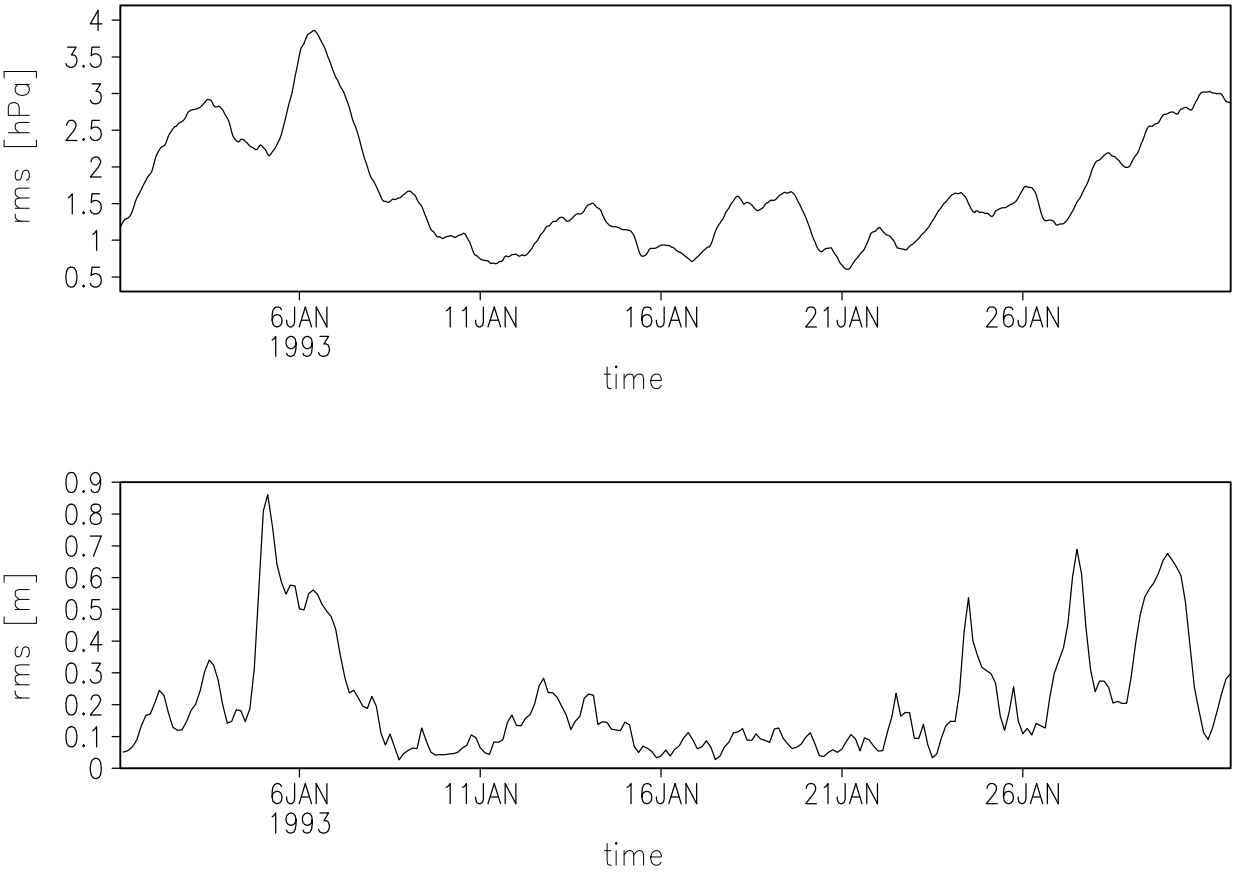

Fig. 2. Root-mean-square (rms) distance for SLP in hPa (top) and Hs in m (bottom) between the ensemble means of the SPN and the CTR ensemble.

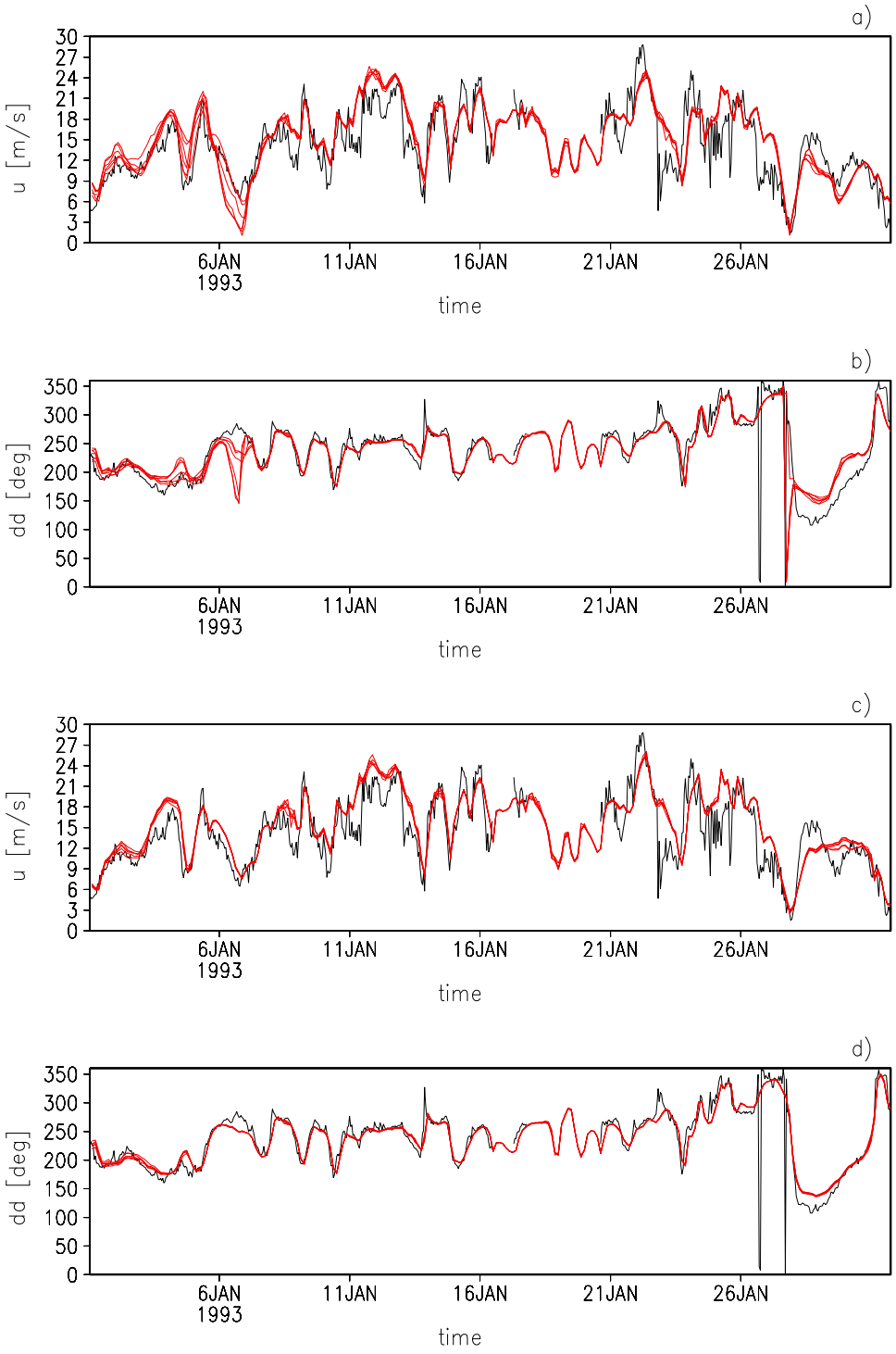

Fig. 3. Observed (black) and simulated (red) wind speed (a, c) in ms^{-1} and wind direction in degrees (b, d) at Ekofisk. The upper two panels (a, b) show the CTR, the lower two panels (c, d) show the SPN simulations.

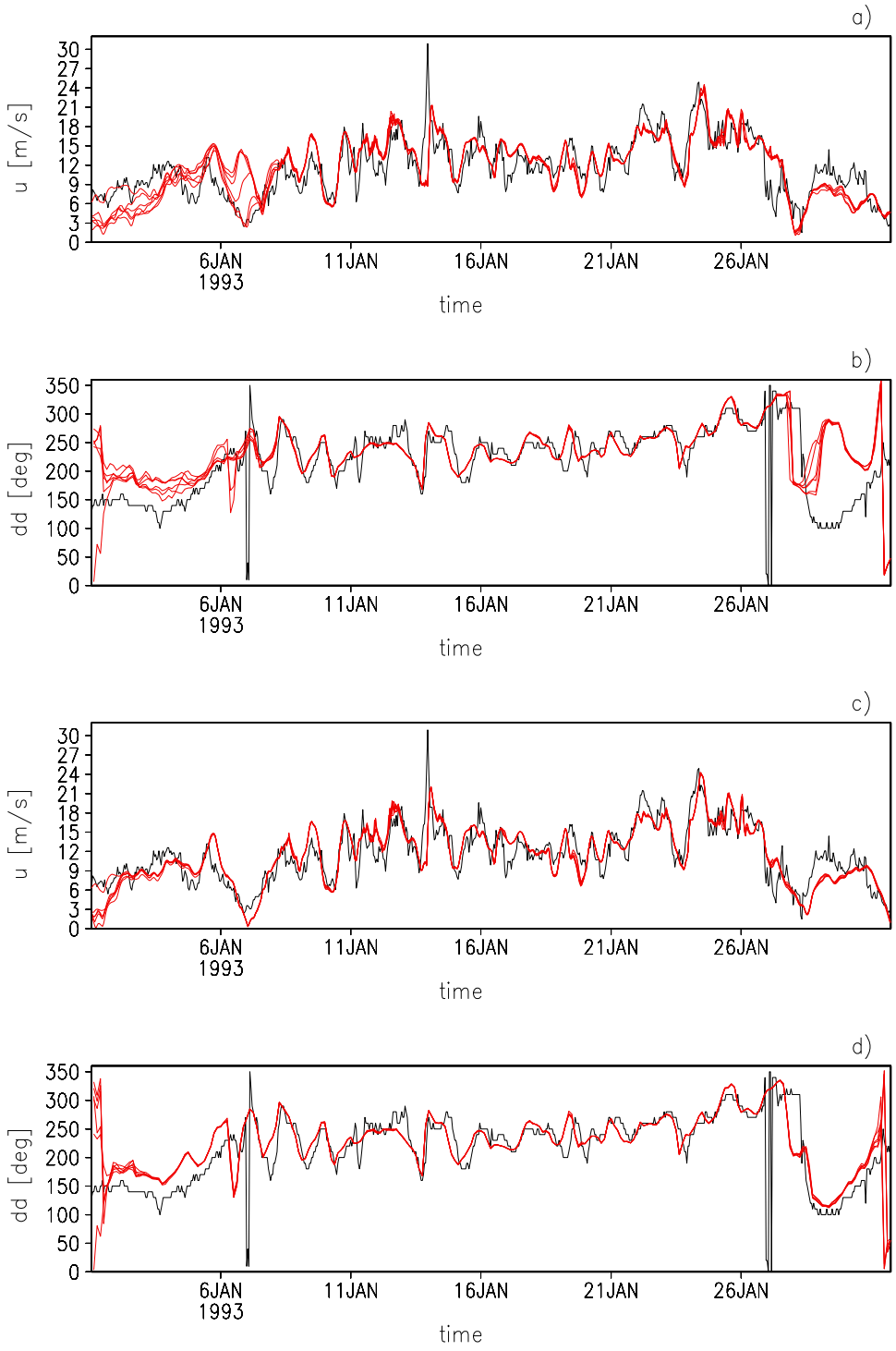

Fig. 4. Observed (black) and simulated (red) wind speed (a, c) in ms^{-1} and wind direction in degrees (b, d) at Scharh¨orn. The upper two panels (a, b) show the CTR, the lower two panels (c, d) show the SPN simulations.

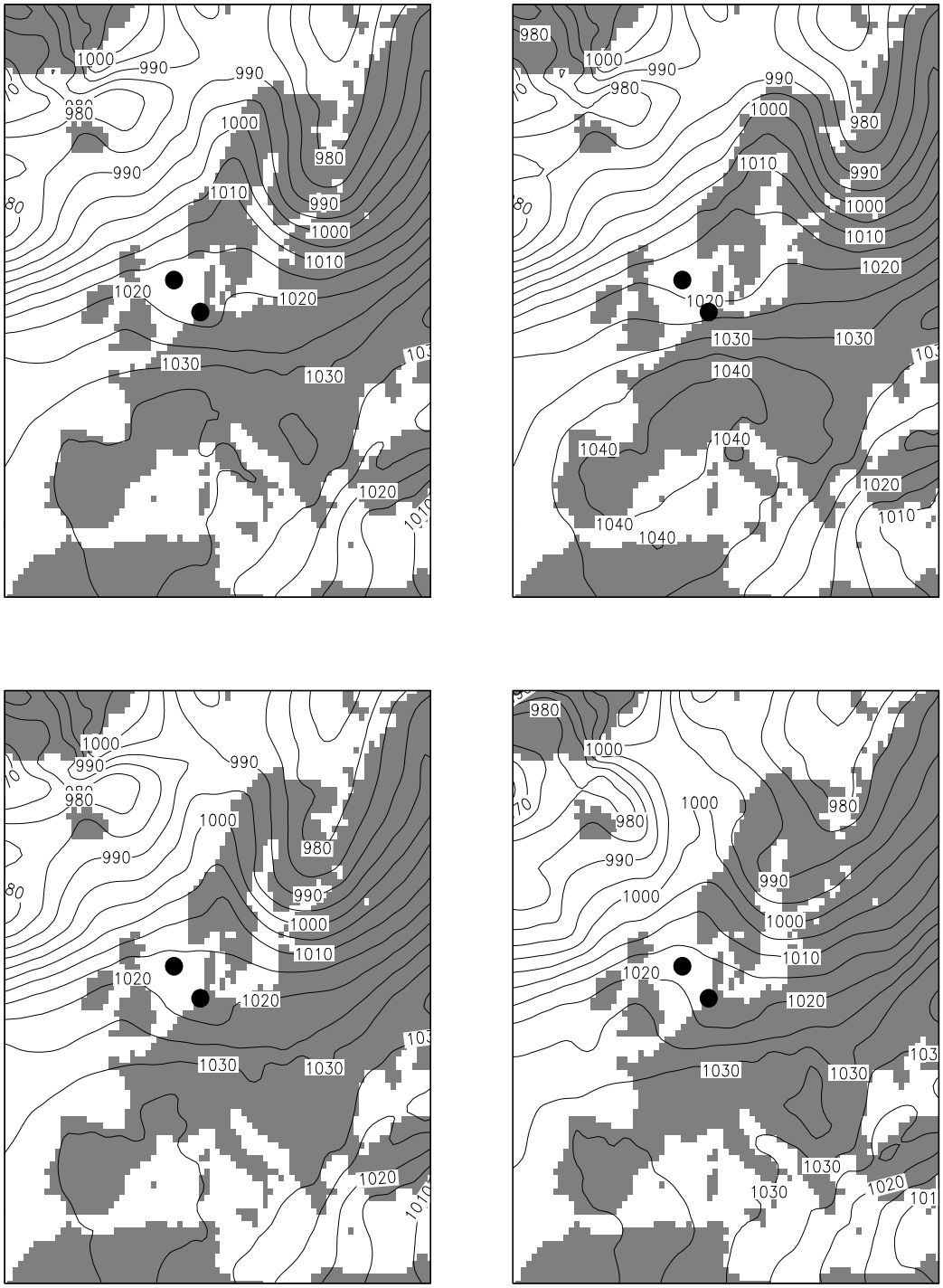

Fig. 5. SLP in hPa for two REMO CTR (upper panel) and one REMO SPN (lower left panel) realizations at 00:00 UTC 7 January 1993 together with the SLP obtained from the routine analysis of the German Weather Service (lower right). The two solid black points in each panel indicate the positions of Ekofisk (northernmost point) and Scharh¨orn (southernmost point).

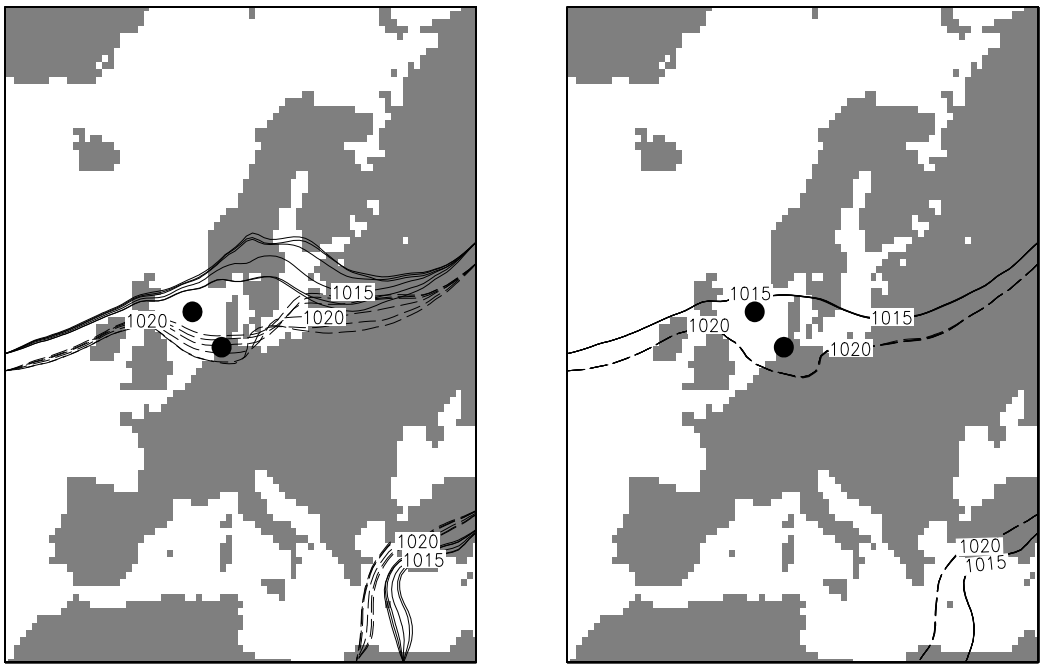

Fig. 6. SLP in hPa obtained from the REMO CTR (left) and the REMO SPN (right) simulations at 00:00 UTC 7 January 1993. Shown are the 1015 hPa (solid) and the 1020 hPa (dashed) contour lines from all 6 REMO CTR (left) and all 6 REMO SPN (right) simulations. Note that the differences are hardly visible for the SPN simulations. The two solid black points indicate the positions of Ekofisk (northernmost) and Scharh¨orn (southernmost points).

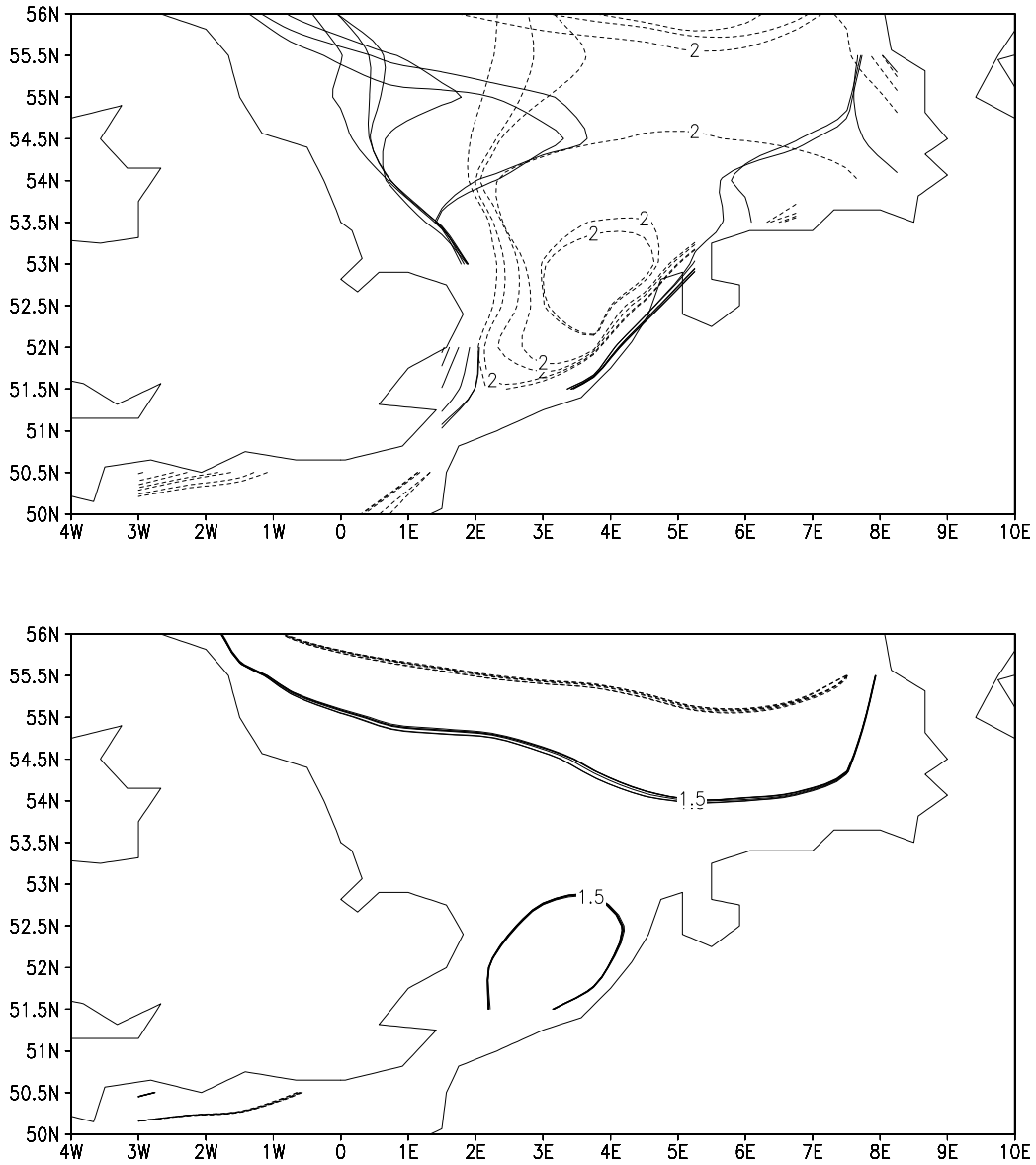

Fig. 7. Total Hs in m for the WAM CTR (upper) and the WAM SPN (lower) simulations at 00:00 UTC 7 January 1993. Shown are the 1.5 m (solid) and the 2.0 m (dashed) contour lines for all 6 WAM CTR (upper) and all 6 WAM SPN (lower) simulations.